High efficiency frequency upconversion of photons carrying orbital angular momentum for a quantum information interface

Ruikai Tang, Xiongjie Li, Wenjie Wu, Haifeng Pan, Heping Zeng and E Wu*

State Key Laboratory of Precision Spectroscopy, East China Normal University, Shanghai, 200062, China
*ewu@phy.ecnu.edu.cn

Abstract: The orbital angular momentum (OAM) of light shows great potential in quantum communication. The transmission wavelength for telecom is usually around 1550 nm, while the common quantum information storage and processing devices based on atoms, ions or NV color centers are for photons in visible regime. Here we demonstrate a quantum information interface based on the frequency upconversion for photons carrying OAM states from telecom wavelength to visible regime by sum-frequency generation with high quantum conversion efficiency. The infrared photons at 1558 nm carrying different OAM values were converted to the visible regime of 622.2 nm, and the OAM value of the signal photons was well preserved in the frequency upconversion process with pump beam in Gaussian profile.

OCIS codes: (190.7220) Upconversion; (230.7405) Optical device, wavelength conversion devices.

References and links

1. L. Allen, M. W. Beijersbergen, R. J. C. Spreeuw, and J. P. Woerdman, "Orbital angular momentum of light and the transformation of Laguerre-Gaussian laser modes," Phys. Rev. A **45**(11), 8185–8189 (1992).
2. D. G. Grier, "A revolution in optical manipulation," Nature **424**(6950), 810–816 (2003).
3. J.-H. Kang, K. Kim, H.-S. Ee, Y.-H. Lee, T.-Y. Yoon, M.-K. Seo, and H.-G. Park, "Low-power nano-optical vortex trapping via plasmonic diabolo nanoantennas," Nat. Commun. **2**, 582 (2011).
4. J. Ng, Z. Lin, and C. T. Chan, "Theory of optical trapping by an optical vortex beam," Phys. Rev. Lett. **104**(10), 103601 (2010).
5. S. Bretschneider, C. Eggeling, and S. W. Hell, "Breaking the diffraction barrier in fluorescence microscopy by optical shelving," Phys. Rev. Lett. **98**(21), 218103 (2007).
6. A. Mair, A. Vaziri, G. Weihs, and A. Zeilinger, "Entanglement of the orbital angular momentum states of photons," Nature **412**(6844), 313–316 (2001).
7. S. Gröblacher, T. Jennewein, A. Vaziri, G. Weihs, and A. Zeilinger, "Experimental quantum cryptography with qutrits," New J. Phys. **8**(5), 75 (2006).
8. R. Fickler, R. Lapkiewicz, W. N. Plick, M. Krenn, C. Schaeff, S. Ramelow, and A. Zeilinger, "Quantum entanglement of high angular momenta," Science **338**(6107), 640–643 (2012).
9. A. C. Dada, J. Leach, G. S. Buller, M. J. Padgett, and E. Andersson, "Experimental high-dimensional two-photon entanglement and violations of generalized Bell inequalities," Nat. Phys. **7**(9), 677–680 (2011).
10. G. Gibson, J. Courtial, M. Padgett, M. Vasnetsov, V. Pas'ko, S. Barnett, and S. Franke-Arnold, "Free-space information transfer using light beams carrying orbital angular momentum," Opt. Express **12**(22), 5448–5456 (2004).
11. J. Wang, J.-Y. Yang, I. M. Fazal, N. Ahmed, Y. Yan, H. Huang, Y. Ren, Y. Yue, S. Dolinar, M. Tur, and A. E. Willner, "Terabit free-space data transmission employing orbital angular momentum multiplexing," Nat. Photonics **6**(7), 488–496 (2012).
12. J. T. Barreiro, T. C. Wei, and P. G. Kwiat, "Beating the channel capacity limit for linear photonic superdense coding," Nat. Phys. **4**(8), 662 (2008).
13. E. Nagali, L. Sansoni, F. Sciarrino, F. De Martini, L. Marrucci, B. Piccirillo, E. Karimi, and E. Santamato, "Optimal quantum cloning of orbital angular momentum photon qubits through Hong-Ou-Mandel coalescence," Nat. Photonics **3**(12), 720–723 (2009).
14. J. C. Garcia-Escartin and P. Chamorro-Posada, "Quantum computer networks with the orbital angular momentum of light," Phys. Rev. A **86**(3), 032334 (2012).

15. M. Mafu, A. Dudley, S. Goyal, D. Giovannini, M. McLaren, M. J. Padgett, T. Konrad, F. Petruccione, N. Lutkenhaus, and A. Forbes, "Higher-dimensional orbital-angular-momentum-based quantum key distribution with mutually unbiased bases," Phys. Rev. A **88**(3), 032305 (2013).
16. A. Nicolas, L. Veissier, L. Giner, E. Giacobino, D. Maxein, and J. Laurat, "A quantum memory for orbital angular momentum photonic qubits," Nat. Photonics **8**(3), 234–238 (2014).
17. D. S. Ding, Z. Y. Zhou, B. S. Shi, and G. C. Guo, "Single-photon-level quantum image memory based on cold atomic ensembles," Nat. Commun. **4**, 2527 (2013).
18. N. Bozinovic, Y. Yue, Y. Ren, M. Tur, P. Kristensen, H. Huang, A. E. Willner, and S. Ramachandran, "Terabit-scale orbital angular momentum mode division multiplexing in fibers," Science **340**(6140), 1545–1548 (2013).
19. P. Kumar, "Quantum frequency conversion," Opt. Lett. **15**(24), 1476–1478 (1990).
20. M. T. Rakher, L. J. Ma, O. Slattery, X. A. Tang, and K. Srinivasan, "Quantum transduction of telecommunications-band single photons from a quantum dot by frequency upconversion," Nat. Photonics **4**(11), 786–791 (2010).
21. X. R. Gu, Y. Li, H. F. Pan, E. Wu, and H. P. Zeng, "High-speed single-photon frequency upconversion with synchronous pump pulses," IEEE J. Sel. Top. Quantum Electron. **15**(6), 1748–1752 (2009).
22. X. R. Gu, K. Huang, Y. Li, H. F. Pan, E. Wu, and H. P. Zeng, "Temporal and spectral control of single-photon frequency upconversion for pulsed radiation," Appl. Phys. Lett. **96**(13), 131111 (2010).
23. K. Huang, X. R. Gu, H. F. Pan, E. Wu, and H. P. Zeng, "Synchronized fiber lasers for efficient coincidence single-photon frequency upconversion," IEEE J. Sel. Top. Quantum Electron. **18**(2), 562–566 (2012).
24. J. S. Pelc, Q. Zhang, C. R. Phillips, L. Yu, Y. Yamamoto, and M. M. Fejer, "Cascaded frequency upconversion for high-speed single-photon detection at 1550 nm," Opt. Lett. **37**(4), 476–478 (2012).
25. P. S. Kuo, J. S. Pelc, O. Slattery, Y. S. Kim, M. M. Fejer, and X. Tang, "Reducing noise in single-photon-level frequency conversion," Opt. Lett. **38**(8), 1310–1312 (2013).
26. D. Li, Y. Jiang, Y. J. J. Ding, I. B. Zotova, and N. S. Prasad, "Approaching single-photon detection in near-infrared region," Appl. Phys. Lett. **101**(14), 141126 (2012).
27. Z. Y. Zhou, D. S. Ding, Y. K. Jiang, Y. Li, S. Shi, X. S. Wang, and B. S. Shi, "Orbital angular momentum light frequency conversion and interference with quasi-phase matching crystals," Opt. Express **22**(17), 20298–20310 (2014).
28. Z. Y. Zhou, Y. Li, D. S. Ding, W. Zhang, S. Shi, B. S. Shi, and G. C. Guo, "Highly efficient second harmonic generation of a light carrying orbital angular momentum in an external cavity," Opt. Express **22**(19), 23673–23678 (2014).
29. Y. Li, Z. Yuan, D. Ding, and B. Shi, "Sum frequency generation with two orbital angular momentum carrying laser beams," J. Opt. Soc. Am. B **32**(3), 407–411 (2015).
30. Y. Li, Z. Yuan, D. Ding, Y. Jiang, X. Wang, S. Shi, B. Shi, and G. Guo, "Orbital angular momentum photonic quantum interface," arXiv: 1410.7543 (2014).
31. J. Leach, M. J. Padgett, S. M. Barnett, S. Franke-Arnold, and J. Courtial, "Measuring the orbital angular momentum of a single photon," Phys. Rev. Lett. **88**(25), 257901 (2002).
32. G. Shao, Z. Wu, J. Chen, F. Xu, and Y. Lu, "Nonlinear frequency conversion of fields with orbital angular momentum using quasi-phase-matching," Phys. Rev. A **88**(6), 063827 (2013).
33. K. Huang, X. R. Gu, H. F. Pan, E. Wu, and H. P. Zeng, "Few-photon-level two-dimensional infrared imaging by coincidence frequency upconversion," Appl. Phys. Lett. **100**(15), 151102 (2012).

1. Introduction

Light with helical phase structures has been widely used in many fields nowadays since the OAM of light was first found by Allen in 1992 [1]. By taking the advantage of its mechanical torque, optical vortices have been used as optical tweezers [2], optical trapping [3,4] to manipulate particles under micrometers. Furthermore, optical vortices are also applied in a 2-D microscope scanning system to obtain the super resolution microscope image [5]. In recent years, following the pioneering work of entanglement in OAM states of light at single-photon level [6], great progress has been made in OAM encoded quantum cryptography [7] and high-dimensional entanglement [8,9]. Besides these ground-breaking experiments on the fundamental research, using the OAM of light as photonic qubits shows great potential in applications of optical communication [10–12], optimal quantum cloning [13], quantum computer networks [14], quantum key distribution [15], and quantum memory [16,17]. However, OAM qubits at optical fiber [18] telecommunication wavelengths around 1550 nm could not match the quantum information storage and processing devices based on atoms, ions or NV color centers that absorb and emit photons at visible wavelengths around 600~700 nm. Single-photon frequency upconversion is thereupon considered to be utilized as a quantum information interface that enables qubits to transfer from infrared to visible regime, while preserving the quantum state information [19,20]. In the last decade, those single-photon upconversion systems have featured the near unit quantum conversion efficiency, low background noise, and quantum state maintaining [20–26] by using a period poled lithium niobate (PPLN) media, providing a possible solution for the quantum information interface for the OAM photons.

Recently, orbital angular momentum carried light transduction based on frequency conversion was demonstrated with different schemes [27–30]. An ultraviolet light with OAM of 100 $\hbar$ was generated by the second-harmonic generation (SHG) with a quasi-phase matching (QPM) crystal [27]. OAM conservation was verified by using a specially designed interferometer. Later, they demonstrated OAM of 2 $\hbar$ beam SHG with 10.3% conversion efficiency when the pump power was 219 mW in an external cavity [28]. And arbitrary sum arithmetic of lights with OAM in upconversion process was reported with the signal light from a Ti: sapphire laser converted in a PPKTP bulk crystal to visible area [29]. Moreover, an orbital angular momentum photonic quantum interface was also proposed to upconvert the heralded single-photon OAM state of 1 $\hbar$ from 1560 nm to 525 nm in an external cavity with 8.33% conversion efficiency at 750 mW pump power [30]. However, the conversion efficiency of these schemes was quite low compared to the near unit efficiency in the single-photon frequency upconversion detection demonstrations [21–25].

In this letter, we demonstrated quantum information interface for photons in the Laguerre-Gaussian (LG) mode with an azimuthal phase dependence. The photons carrying OAM at a telecom wavelength of 1558.0 nm were transferred to visible wavelength of 622.2 nm by sum-frequency generation (SFG) in a PPLN bulk crystal at single-photon level. Different from the previous experimental demonstration, we used synchronized pulsed pumping upconversion system, achieving a high quantum conversion efficiency of 68% with photons carrying OAM value of 1$\hbar$ and the background noise was as low as 3.8×10^3 cps. The OAM value of SFG output was measured by a Mach-Zehnder (M-Z) interferometer with a Dove prism in one of the interferometer arm [31], verifying that the OAM of the signal photons was well conserved while converted by a Gaussian pump beam in the frequency upconversion process. LG modes are exploited to represent the beams with OAM, which are characterized by the azimuthal index l. In such LG mode beams with an azimuthal phase dependence in form of $\exp(il\phi)$, each photon carries an OAM of $l\hbar$, which is the useful freedom degree in quantum communication for encoding.

Considering the QPM frequency upconversion that the infrared photons at λ_1 are converted to visible wavelength of λ_3 in a nonlinear $\chi^{(2)}$ crystal under a strong pump field $\boldsymbol{E_2}$ of wavelength of λ_2.The solution to the coupled mode equations for the single-photon frequency upconversion can be depicted as

$$\hat{a}_1(L) = \hat{a}_1(0)\cos(\gamma E_2 L) - \hat{a}_3 \sin(\gamma E_2 L), \tag{1}$$

$$\hat{a}_3(L) = \hat{a}_1(0)\sin(\gamma E_2 L) + \hat{a}_3 \cos(\gamma E_2 L), \tag{2}$$

where $\hat{a}_i$ is the annihilation operator, L is the crystal length, and γ is the nonlinear interaction strength. When the values for the pump field $\boldsymbol{E_2}$ and the nonlinear interaction strength γ are large enough to fulfill $|\gamma E_2 L| = \pi/2$ in Eqs. (1) and (2), the quantum states at wavelength λ_1 can be translated to the same quantum states at λ_3 with unity quantum conversion efficiency. Besides the conservations of energy and momentum, the OAM value could be well conserved in the frequency upconversion process [27–30, 32], providing a quantum interface to connect the telecom channels and quantum storage devices which are using OAM encoding.

#236046 - $15.00 USD Received 11 Mar 2015; revised 1 Apr 2015; accepted 2 Apr 2015; published 8 Apr 2015

2. Experiment setup

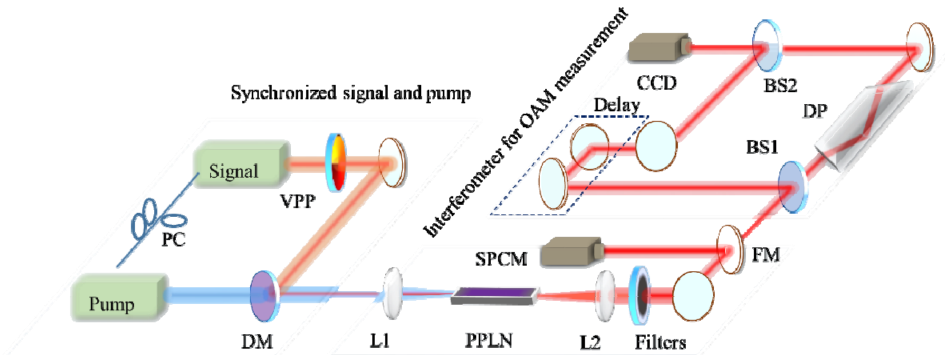

Fig. 1. Schematic of experimental setup. PC: polarization control; VPP, vortex phase plate; DM: dichronic mirror; L1,2: Lenses; PPLN: period poled lithium niobate; FM: flip mirror; SPCM: single photon counting module; BS1,2: beam splitters; DP: dove prism; CCD: charge coupled device camera.

Figure 1 outlines the experimental setup of the quantum interface for photons carrying OAM states. The scheme was consisted of a synchronized pulsed signal and pump source, a single-photon frequency upconversion system, and an interferometer for OAM verification. The signal and pump sources included two synchronized fiber pulse lasers (for the signal and pump source). The two fiber lasers were synchronized in master-slave configuration [21]. The master and slave lasers were an erbium-doped fiber laser (EDFL) and an ytterbium-doped fiber laser (YDFL), respectively. They were passively mode-locked by nonlinear polarization rotation effect. The repetition rate of YDFL was the same with that of the EDFL at 20.3 MHz. The mode-locking of the YDFL was started by injecting the amplified part of the EDFL's output to the fiber cavity of YDFL to induce the cross phase modulation based on the nonlinear polarization rotation, thus the YDFL was synchronized to the EDFL [22,23]. The other part of the output from the EDFL, acting as the signal, was filtered by a fiber Bragg grating (FBG) to fulfill the acceptance bandwidth of the PPLN crystal. The spectral bandwidth of the signal was 0.5 nm with the center wavelength of 1558.0 nm, and the pulse duration of the signal was 12.4 ps. The signal pulse was attenuated to contain ~0.06 photons per pulse. The spectrum of the pump laser was also filtered by an FBG at 1035.9 nm with bandwidth of 0.3 nm. The pump laser could provide a maximum average power of 213 mW by a two-step amplification of the output of YDFL. The pulse duration of pump source was 31.4 ps, so that the corresponding signal pulse could be wholly enveloped to achieve high conversion efficiency.

Before the signal was injected to the single-photon frequency upconversion system, a vortex phase plates (VPP) (VPP-1c,RP Photonics) was inserted to the signal beam to generate a LG mode beam with OAM of $l\hbar$. The signal was combined with the pump laser by a dichroic mirror. The polarizations of the pump and signal pulses were adjusted independently by half wave-plates, and enforced to be the same by a Glan prism to satisfy the Type 0 QPM condition in the PPLN bulk crystal. The length of the PPLN crystal was 50 mm, allowing a long interaction distance of the signal photons with the pump pulses. The signal and pump beams were focused at the center of the PPLN crystal by a lens of 100-mm focal length. The operation temperature of the PPLN crystal was set at 111.3 °C with a fluctuation less than 0.1 °C. The inverse period of the PPLN crystal was 11.0 μm for accomplishing the QPM condition of the SFG. We finely tuned the time delay between the signal and pump pulse to obtain the temporal overlap, ensuring that the signal pulse would interact with the corresponding pump pulse in the PPLN crystal. Then the infrared signal was converted to visible light by SFG. The center

#236046 - $15.00 USD Received 11 Mar 2015; revised 1 Apr 2015; accepted 2 Apr 2015; published 8 Apr 2015

wavelength of SFG photons was 622.2 nm with bandwidth of 0.12 nm. The SFG was steered to pass through series of spectral filters before arriving at a flip-flap mirror. When the mirror was flipped on, the SFG light was coupled into a single-photon counting module (SPCM) (SPCM-AQR-14, PerkinElmer). Otherwise, it would be injected to the interferometer for OAM verification. The balanced M-Z interferometer was specially designed for OAM verification by inserting a Dove Prism into one arm to obtain the interference of the incoming light with its own mirror image. A delay line was set in the other arm to balance the optical delay induced by the Dove prism. Then the photons from the two arms were coupled by a beam splitter BS2 before captured by an electron multiplying CCD camera (iXon3 897, Andor), which was thermoelectrically cooled to −85 °C to lower the dark noise.

3. Results

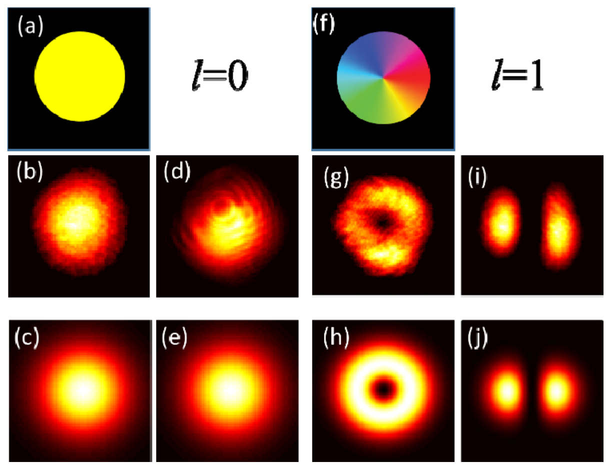

Fig. 2. (a) the constant phase of a Gaussian beam with OAM value of 0; (b) and (c) the experimental and simulated intensity images of SFG output carrying OAM value of 0; (d) and (e) are the experimental and simulated images of SFG output interferometer pattern of the beam in (b) and (c); (f) the phase of the Vortex Phase Plate used to generate the LG beam; (g) and (h) experimental and simulated images of SFG output carrying OAM value of $\hbar$; (i) and (j) are the experimental and simulated images of SFG output interferometer pattern of the beam in (g) and (h).

At the beginning, the OAM value l was 0 for the signal, which was a Gaussian beam in space. The phase of the wavefront was shown in Fig. 2(a). The generated SFG beam was also in Gaussian profile captured by the CCD camera as shown in Fig. 2(b). When the M-Z interferometer was closed, the interference image acquired by the CCD was the constructive pattern of the SFG output shown in Fig. 2(d), matching well with the simulated results in Fig. 2(e). Then we adjusted the VPP to obtain the photons carrying OAM of $1\hbar$ as shown in Fig. 2(f). The intensity distribution of the SFG was depicted in Fig. 2(g), which was an optical ring with no photons at the center as simulated in Fig. 2(h). The interference pattern of the SFG output in Fig. 2(i) implied the OAM value of $1\hbar$, matching well with the theoretical simulation of Fig. 2(j). It is proved that the OAM value was conserved in the SFG nonlinear effect process, showing that this system based on single-photon frequency upconversion could be employed successfully in the translation of infrared telecom OAM photons to the visible wavelengths while preserving very well the OAM value. Moreover, the intensity overlap between the theory and experiment was calculated by

$$F = \iint \sqrt{I_{theory}} \sqrt{I_{exp}} \, \mathrm{d}x\mathrm{d}y, \tag{3}$$

#236046 - $15.00 USD Received 11 Mar 2015; revised 1 Apr 2015; accepted 2 Apr 2015; published 8 Apr 2015

where I_{theory} and I_{exp} are the normalized theory and experimental intensity distribution function, respectively, and x, y were the positions. Obtained from Eq. (3), for the OAM value of 0, the overlap was as high as 95.2%. When the OAM value increased to be $1\hbar$, the overlap dropped a little to be 94.3% due to the beam size mismatch of the pump and the signal in the PPLN crystal.

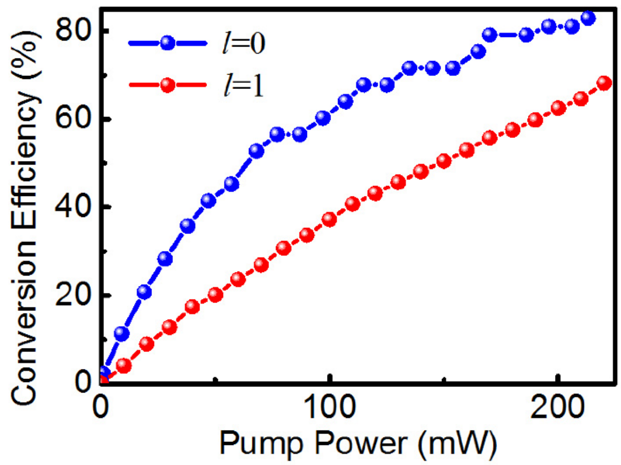

Fig. 3. Quantum conversion efficiency of signal photons carrying OAM 0 (blue line) and 1 $\hbar$ (red line) as a function of the pump power.

Then, the converted output photons were steered to the SPCM for quantum conversion efficiency evaluation. Considering that the total transmittance η_T of the combined filters in front of the SPCM was about ~42% and the quantum efficiency η_D of the SPCM was 60% with dark counts of about 200 cps at 622.2 nm, the maximum conversion efficiency of the Gaussian input signal was 82.9% when the pump power reached 213 mW, corresponding to a peak power of 0.33 kW. The conversion efficiency for $l = 0$ (blue line in Fig. 3) illustrated that the increase of the conversion efficiency became slower and then flattened when the pump power was beyond 150 mW. It is foreseeable that with the pump power further increased, the periodical oscillation of the quantum conversion efficiency dependent on the pump power would appear. However, with the photons carrying OAM of $1\hbar$, a decrease in the quantum conversion efficiency was observed in the red curve in Fig. 3. The maximum quantum conversion efficiency was obtained to be 68% when the pump power reached the maximum of 213 mW. Compare to the high conversion efficiency of the Gaussian beam with OAM value of 0, we found that the decrease of the quantum conversion efficiency for the photons with OAM value of $1\hbar$ was caused mainly by the spatial redistribution of signal intensity induced by the VPP and the difference of energy profile between a Gaussian and a LG beams. Besides, a long PPLN bulk crystal was adopted to obtain a high conversion efficiency. Since the dimension of the crystal was $50 \times 0.9 \times 0.5$ mm^3, the angular acceptance was much limited with such a thickness and length [33]. Therefore, when the beam size of the signal increased due to the spatial phase modulation by the VPP to higher OAM modes, the conversion efficiency decreased because of the non-perfect overlap of the signal beam with the pump beam in the crystal.

In quantum information techniques, the quantum states are quite sensitive to the environmental noise, especially for the quantum states translation. Therefore, we evaluated the noise of the system with the SPCM by blocking the signal beam. As shown in Fig. 4, with the increase of the pump laser power, the noise of the system increased due to the parametric fluorescence induced by the strong pump field in the PPLN crystal [21, 23]. But thanks to the synchronized pulsed pump system, the noise of the system was only 3.8×10^3 cps even at the

#236046 - $15.00 USD Received 11 Mar 2015; revised 1 Apr 2015; accepted 2 Apr 2015; published 8 Apr 2015

maximum pump power of 213 mW, corresponding to only 1.9×10^{-4} noise photons per pulse. Figure 4 illustrated the signal to noise ratio of LG modes $l = 0$ (red) and $l = 1$ (blue). When the pump power increased from 0 to 60 mW, the SNR raised rapidly for the quantum conversion efficiency increased sharply. Beyond that, the SNR of Gaussian beam decreased as the conversion efficiency became saturated. For LG beam $l = 1$, the SNR was stable as the conversion efficiency linearly increased with the pump power. At the maximum pump power, the SNR was still as high as about 50:1.

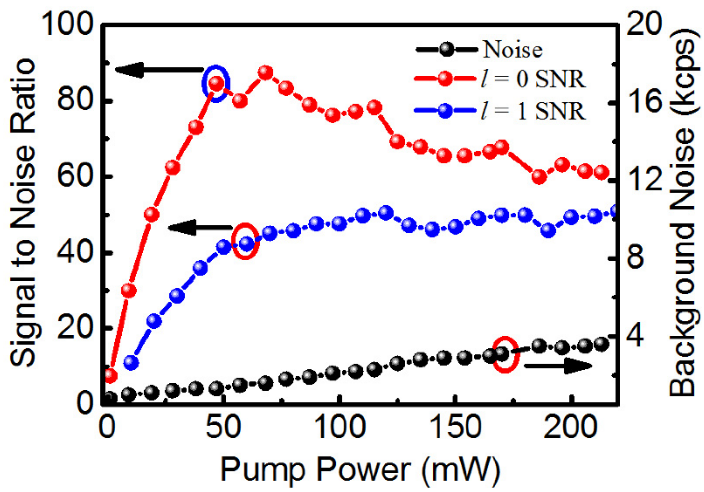

Fig. 4. Signal to noise ratio for different OAM value beams (Left) and the background noise (Right) as a function of the pump power.

4. Discussion

In summary, we demonstrate the high efficiency frequency upconversion of photons carrying orbital angular momentum for a quantum information interface. Photons carrying OAM of $1\hbar$ were converted from telecom wavelength to the visible regime with 68% quantum conversion efficiency, which could be potential applied in quantum information techniques using OAM encoding of the photons. Further research should be done to improve the system toward high efficiency and high speed to fulfill the requirement of a practical quantum interface to connect the quantum communication and quantum memory.

Acknowledgments

This work was funded in part by National Natural Science Foundation of China (61127014, and 61378033), National Key Scientific Instrument Project (2012YQ150092), the Program of Introducing Talents of Discipline to Universities under Grant B12024, Shanghai Rising-Star Program (13QA1401300), and the Shanghai International Cooperation Project (13520720700).